

RESEARCH

Open Access



Morusin shows potent antitumor activity for melanoma through apoptosis induction and proliferation inhibition

Wei Liu^{1,2,3}, Yacong Ji^{1,2}, Feng Wang^{2,3}, Chongyang Li⁴, Shaomin Shi^{1,2,3}, Ruochen Liu², Qian Li^{1,2,3}, Leiyang Guo^{1,2}, Yaling Liu^{1*} and Hongjuan Cui^{2,3,5*}

Abstract

Background The discovery of new anti-melanoma drugs with low side effect is urgently required in the clinic. Recent studies showed that morusin, a flavonoid compound isolated from the root bark of *Morus Alba*, has the potential to treat multiple types of cancers, including breast cancer, gastric cancer, and prostate cancer. However, the anti-cancer effect of morusin on melanoma cells has not been investigated.

Methods We analyzed the effects of morusin on the proliferation, cell cycle, apoptosis, cell migration and invasion ability of melanoma cells A375 and MV3, and further explored the effects of morusin on tumor formation of melanoma cell. Finally, the effects of morusin on the proliferation, cycle, apoptosis, migration and invasion of A375 cells after knockdown of p53 were detected.

Results Morusin effectively inhibits the proliferation of melanoma cells and induces cell cycle arrest in the G2/M phase. Consistently, CyclinB1 and CDK1 that involved in the G2/M phase transition were down-regulated upon morusin treatment, which may be caused by the up-regulation of p53 and p21. In addition, morusin induces cell apoptosis and inhibits migration of melanoma cells, which correlated with the changes in the expression of the associated molecules including PARP, Caspase3, E-Cadherin and Vimentin. Moreover, morusin inhibits tumor growth in vivo with little side effect on the tumor-burden mice. Finally, p53 knockdown partially reversed morusin-mediated cell proliferation inhibition, cell cycle arrest, apoptosis, and metastasis.

Conclusion Collectively, our study expanded the spectrum of the anti-cancer activity of morusin and guaranteed the clinical use of the drug for melanoma treatment.

Keywords Morusin, Melanoma, p53, Proliferation, Apoptosis, Metastasis

*Correspondence:

Yaling Liu
yzling_liu1214@126.com
Hongjuan Cui
hcui@swu.edu.cn

Full list of author information is available at the end of the article



© The Author(s) 2023. **Open Access** This article is licensed under a Creative Commons Attribution 4.0 International License, which permits use, sharing, adaptation, distribution and reproduction in any medium or format, as long as you give appropriate credit to the original author(s) and the source, provide a link to the Creative Commons licence, and indicate if changes were made. The images or other third party material in this article are included in the article's Creative Commons licence, unless indicated otherwise in a credit line to the material. If material is not included in the article's Creative Commons licence and your intended use is not permitted by statutory regulation or exceeds the permitted use, you will need to obtain permission directly from the copyright holder. To view a copy of this licence, visit <http://creativecommons.org/licenses/by/4.0/>. The Creative Commons Public Domain Dedication waiver (<http://creativecommons.org/publicdomain/zero/1.0/>) applies to the data made available in this article, unless otherwise stated in a credit line to the data.

Background

In the past few decades, the incidence of melanoma has been increasing [1]. Melanoma is a skin cancer with a high mortality rate. Although the incidence of melanoma only accounts for about 3% of all malignant tumors, due to its rapid progression, strong lymphatic and distant metastasis ability [2–4] and poor prognosis, its mortality accounts for 90% of the mortality of skin tumors [5], and the survival time of patients with systemic metastasis is less than 1 year [4]. Current treatments include surgical excision, drug treatment, chemotherapy, targeted therapy and immunotherapy [6]. However, most of the anti-melanoma drugs commonly used in clinical practice have serious adverse reactions. Therefore, the development of new anti-melanoma drugs is an urgent problem at the present stage.

In recent years, it has been discovered that natural compounds, such as flavonoids, polyphenols, and alkaloids [7], have good killing effects on tumor cells, while little effect on normal cells and few adverse reactions [6]. Luteolin (3,4,5,7-tetrahydroxy flavone) is a flavonoid found in different plants, such as vegetables and fruits [8]. Studies have found that it has anti-inflammatory, anti-allergic, anti-anxiety, neuroprotective and anti-cancer effects [8–10]. Luteolin inhibits the proliferation [11] and induces the apoptosis of A375, human melanoma cells, by reducing the expressions of MMP-2 and MMP-9 through the PI3K/AKT pathway [12]. In addition, luteolin significantly inhibits the migration, invasion, adhesion and microtubule formation potential of highly metastatic A375 and B-16-F10 melanoma cells with no significant cytotoxicity [13]. Resveratrol, a polyphenol component, is found in grapes and some other plants. It has anti-cancer properties [14] and can significantly inhibit the proliferation of melanoma cells [15, 16], induce apoptosis by up-regulating p53 in a concentration-dependent manner [16], inhibit cell migration [17] and murine melanoma tumor growth [18]. Berberine is an isoquinoline alkaloid present in several plants, and it has anti-cancer activity and less toxic to normal cells [19]. Berberine can induce cell morphological changes, inhibit migration and invasion of A375 cells [20]. Morusin is one of the isoprene flavonoid derivatives from the root bark of *Morus* (Fig. S1A). Recent studies have reported that morusin exhibits anti-tumor biological activity in many human cancers. In human gastric cancer, morusin inhibits cell proliferation and tumor growth by down-regulating c-Myc [21]. Morusin induces autophagy by activation of AMPK and inhibition of mTOR activity in HeLa cells [22], and induces apoptosis in human colorectal cancer cells through NF- κ B pathway [23]. Morusin could inhibit renal carcinoma cell growth and migration, induce cell apoptosis through the mitogen-activated protein kinase

(MAPK) signaling pathway [24]. In human non-small cell lung cancer and human hepatocellular carcinoma, morusin can induce apoptosis through EGFR/STAT3 or IL-6/STAT3 signaling pathway to play an anti-cancer effect [25, 26].

As we all know, p53 is a transcription factor that regulates many cell pathways, such as cell cycle, DNA damage, apoptosis, autophagy and cell metabolism. Loss of p53 expression can down-regulate BubR1, damage part of the function of the spindle checkpoint, and lead to the occurrence and development of colorectal cancer [27]. In addition, p53 not only plays an important role in cancer, but also has a regulatory function in lung fibrosis and adipogenesis [28, 29]. Due to its more functions, p53 is considered an important target for the development of new anti-cancer treatment strategies.

Our study is the first to demonstrate the anti-tumor effect of morusin in melanoma, which inhibits cell proliferation, induces cell cycle arrest, promotes apoptosis, and inhibits cell migration and invasion by increasing the expression of p53. These results illustrate the anti-melanoma effect of morusin and the underlying mechanism, suggesting potential clinical usage of the drug.

Methods

Cell culture

The human melanoma cell lines (A375 and MV3), PIG1 melanocytes, and the human embryonic renal cell line 293FT were purchased in American Type Culture Collection (ATCC, Manassas, VA, USA). HaCaT keratinocytes were purchased from Cell Line Service GmbH. These cells were stored in our laboratory. A375, PIG1, and HaCaT cells were cultured in Dulbecco's modified Eagle's medium (DMEM, Gibco, New York, NY, USA). Roswell Park Memorial Institute-1640 (RPMI-1640, Gibco) was used for maintaining MV3 cells. The 293FT cells were cultured as described previously [30]. They were supplemented with 10% fetal bovine serum (FBS, Gibco), 1% penicillin and streptomycin (P/S, Invitrogen, California, CA, USA). All cells were cultured at 37°C in a humidified incubator with 5% CO₂.

Morusin treatment

Morusin was purchased from Must Bio-Technology Co., Ltd. (Cat. No.:62596–29-6; Chengdu, China) and then dissolved in DMSO as 100 mM stock solution. The human melanoma cell lines, A375 and MV3 were treated with morusin in different concentrations (2, 5 and 10 μ M were used in A375 cells, and 5, 10 and 15 μ M were used in MV3 cells). In our experiments, DMSO was used as control group. Maintained for different times (0, 12, 24 and 36 h), A375 cells were treated with 5 μ M morusin,

and MV3 cells were treated with 10 μ M morusin. Each experiment was repeated three times.

Transfection and infection

The plasmid shp53(1#, 3#) and shGFP were purchased from Sigma-Aldrich as described previously [30]. According to manufacturer's instructions, first, liposomes and packaging plasmids (PLP1, PLP2, VSVG, target plasmids: shGFP, shp53 1#, shp53 3#) were transfected into 293FT cells. After 8 h, the old medium was removed, and fresh 293FT medium was added. After 48 h, the viral supernatant was collected and used to infect the melanoma cell line A375. Then the positive cells were screened by puromycin.

Cell viability assays

The IC₅₀ of melanoma cells A375 and MV3, as well as PIG1 and HaCaT cells, was determined by MTT assay. By using the hemocytometer, the number of cells in each well of 96-well cell culture plate was 1000. After incubating with different doses of morusin (0.001 \times 0.01 \times 0.1 \times 1 \times 10 \times 20 \times 40 \times 60 \times 80 and 160 μ M) or DMSO for 24 h, 20 μ L of MTT (5 mg/mL, Sigma Aldrich, USA) staining solution was added into each well, which was put back to 37°C and cultured in 5% CO₂ incubator. After 1 h, the old medium was removed. And 200 μ L of DMSO was added into each well to determine the absorbance at 490 nm by the Thermo Science Microplate Reader. We analyzed the data through GraphPad Prism 8.3.0. Each experiment was repeated three times.

BrdU staining

The number of cells per well was 4×10^4 in the 24-well plate, and the cells were cultured in 500 μ L medium (DMEM for A375 and RPMI-1640 for MV3) for 12 h in the cell culture chamber. Then morusin (5 μ M of morusin was added to A375, 10 μ M of morusin was added to MV3) was added to medium, and DMSO was added to the control group for 24 h. The detailed steps of the following experimental methods were described in the previous article [31]. Finally, photos were taken under the microscope and at least 10 randomly selected regions were analyzed for BrdU positive cells.

Flow cytometry analysis

After A375 cells were treated with 2 or 5 μ M morusin, MV3 cells were treated with 5 or 10 μ M morusin (equal volume of DMSO was used to control) for 24 h, the cells were washed 3 times with pre-cooling PBS. For the cell cycle assay, the cells were suspended in 75% ethanol at 4°C for 24 h. After that, cells were washed with PBS buffer, then incubated with propidium iodide (PI) containing with RNase A (Sigma Aldrich, USA) at 37°C for

1 h in dark. Cells were collected by the FACS C6 (BD, USA) and the data was analyzed with Cell Quest software. For the cell apoptosis assay, the cells were resuspended in 100 μ L binding buffer with 5 μ L Annexin V and 5 μ L propidium iodide (PI), culturing for 30 min [32]. Then the cells were collected by the FACS C6 and the data was analyzed by using the Cell Quest software. Each experiment was repeated three times.

Western blot analysis

A375 and MV3 cells were collected and then lysed with RIPA lysis buffer, which contained phenyl methane sulfonyl fluoride (PMSF). Then BCA protein assay kit (Beyotime Biotech, China) was used to measure protein concentration. The proteins were separated by 10% or 12% SDS-PAGE, and then transferred to a polyvinylidene difluoride membrane. After blocking with 5% defatted milk for 2 h, the membrane was cut according to the size of marker. The membrane was incubated with primary antibody against p53 (1:1000, Proteintech, China, 10,442-1-AP), p21 (1:1000, Proteintech, China, 10,355-1-AP), CyclinB1 (1:1000, Cell Signaling Technology, CST, USA, #12,231), CDK1 (1:2000, Abcam, USA, ab245318), PARP (1:1000, Cell Signaling Technology, CST, USA, #9542), Caspase3 (1:1000, Cell Signaling Technology, CST, USA, #9662), MMP2 (1:1000, Proteintech, China, 10,373-2-AP), E-Cadherin (1:1000, Proteintech, USA, 20,874-1-AP), Vimentin (1:1000, Proteintech, USA, Catalog number: 10366-1-AP), Tubulin (1:1000, Cell Signaling Technology, CST, USA, #2144) at 4°C overnight. After washing with TBST buffer for 3 times, the membrane was incubated with HRP-conjugated secondary antibody (goat anti-rabbit IgG and goat anti-mouse IgG, 1:10,000, Life Technology, USA) for 2 h at room temperature. Then the proteins bands were finally visualized and captured by the detection analysis system (Clix Science, China). Unfortunately, we lack images of sufficient length.

Wound-healing assays

The detailed experimental method has been reported in the previous literature [33–35]. In brief, 1×10^6 cells were planted in each well of the 6-well plate. When the cells were overgrown, we scratched them by the tip of a white spear and washed them with PBS. Finally, serum-free medium with morusin (A375 cells were used 2 and 5 μ M, MV3 cells were used 5 and 10 μ M) or DMSO was added to cells. Observed the migration of cells in the exposed area and took pictures at indicated time.

Cell migration and invasion

Briefly, a total of 5×10^5 cells were added into multiporouspolycarbonate membrane insert (8- μ m pore size) (Corning), which were fitted into a 24-well plate for cell

migration assays. Added 200 μ L 1% serum medium to the inside and 500 μ L 10% FBS medium to the outside as the infiltrating agent. DMEM medium contained 5 μ M morusin or DMSO. 1640 medium contained 10 μ M morusin or DMSO. After the 24-well plate was placed in an incubator at 37°C (A375 cells were cultured for 12 h, MV3 cells were cultured for 24 h), the chamber was washed with PBS solution 3 times, and 4% paraformaldehyde was added to fix it for 20 min. Washed once with PBS solution and put it into 1 mL crystal violet staining solution for 20 min. After gently wiping the bottom with cotton, we observed and took pictures with the microscope. The transwell invasion assays were performed under the same conditions as the transwell migration assays, but the top chamber was added 50 μ L matrigel (10 mg/mL, Corning), then incubated for 72 h. Each experiment was repeated three times.

Soft agar colony formation assay

The effect of morusin on the colony formation ability of melanoma cells was determined by soft agar assay. In short, 2×DMEM/RPMI 1640 medium (DMEM medium for A375 cells, and RPMI 1640 medium for MV3) was mixed with 1.2% low-melting-point agarose in a 1:1 ratio to make the base agar, and added 1 mL to a 6-well plate. 1000 of A375 or MV3 cells were mixed with 1.5 mL DMEM/RPMI 1640 medium containing 0.3% agarose with morusin (5 μ M, 10 μ M or DMSO) and added to the top of base agar. Generally, after 3 weeks, the images were collected by white light microscope. Then 200 μ L MTT staining solution was added into each well. Finally, imaging and counting were performed after the reaction at 37°C for 30 min.

Animal studies

Animal experiments were approved by the animal ethics committee of Southwest University (Chongqing, China). Three-week-old female mice (NOD/SCID) were purchased and housed in SPF room for 1 week before injection. Then 1×10^6 MV3 cells in 100 μ L PBS were subcutaneously injected to flanks of mice. After one week, the mice were randomly divided into two groups. One group was intraperitoneally injected with morusin (25 mg/kg) and another group was injected with DMSO as control every 2 days for 20 days. In the meantime, the mice weight and tumor volume (tumor volume = length \times width² \times ($\pi/6$)) were measured every 2 days. After three weeks, the tumors were collected and fixed with paraformaldehyde. Then hematoxylin–eosin (H&E) and immunohistochemistry (IHC) experiments were performed. Finally, we injected Avertin and euthanized the mice by cervical dislocation.

Vector construction and transfection

pLKO.1 expressing p53 short hairpin RNA (shp53) were constructed by using the double strand of shRNAs below. shp53 1#: F: CAGCACATGACGGAGGTTGT; R: TCA TCCAAATACTCCACACGC. shp53 3#: F: ACAGCT TTGAGGTGCGTGTTT; R: CCCTTTCTTGCGGAG ATTCTCT.

Quantitative real-time PCR (qRT-PCR)

Cells were collected after treatment with DMSO or morusin at 37 °C for 24 h. Total RNA was isolated from the cells using TRIzol reagent (Invitrogen, Carlsbad, CA, USA) according to the manufacturer's instructions. Reverse transcription was performed using M-MLV reverse transcriptase (Promega, Madison, WI, USA). Quantitative real-time fluorescent quantitative PCR (qRT-PCR) was used to detect the relative expression of the p53 gene.

Statistics analysis

All experiments were confirmed by three independent experiments. All data were analysed by GraphPad Prism 8.3.0. In this study, quantitative data were expressed as the mean \pm standard deviation. One-way ANOVA was used to assess the mean difference among three or more groups, further multiple comparisons were done with Tukey's test, and two-tailed Student's t-test was performed for paired samples, $P < 0.05$ was considered as statistically significant (* $P < 0.05$, ** $P < 0.01$, *** $P < 0.001$).

Results

Morusin inhibits cell proliferation in melanoma cells

In order to explore the viability effect of morusin in melanoma cells, we performed IC₅₀ assay by 10 different doses of morusin treatment for 24 h in A375 and MV3 cells, and the results showed that the IC₅₀ of morusin in A375 is 4.634 μ M and MV3 is 9.7 μ M (Fig. 1A and B). Meanwhile, the IC₅₀ of morusin for PIG1 and HaCaT cells were 21.04 and 18.01 μ M, which were higher than that of melanoma cells (Fig. S1C and D). Next, the human melanoma A375 and MV3 cells were treated with different concentrations of morusin for 24 h. By the microscope, we found that the obvious changes in the morphology of the cells after morusin treatment, and the number of cells decreased in a dose-dependent manner as well (Fig. 1C and D). MTT assay also showed that comparing with DMSO group, A375 cells treated with 5 and 10 μ M, MV3 cells treated with 10 and 15 μ M morusin had sharp decline in cell growth curve (Fig. 1E and F). Besides, 10 μ M morusin has no significant effect on cell viability of PIG1 and HaCaT cells (Fig. S1E and F). Dacarbazine (DTIC) is the first generation of drug approved by

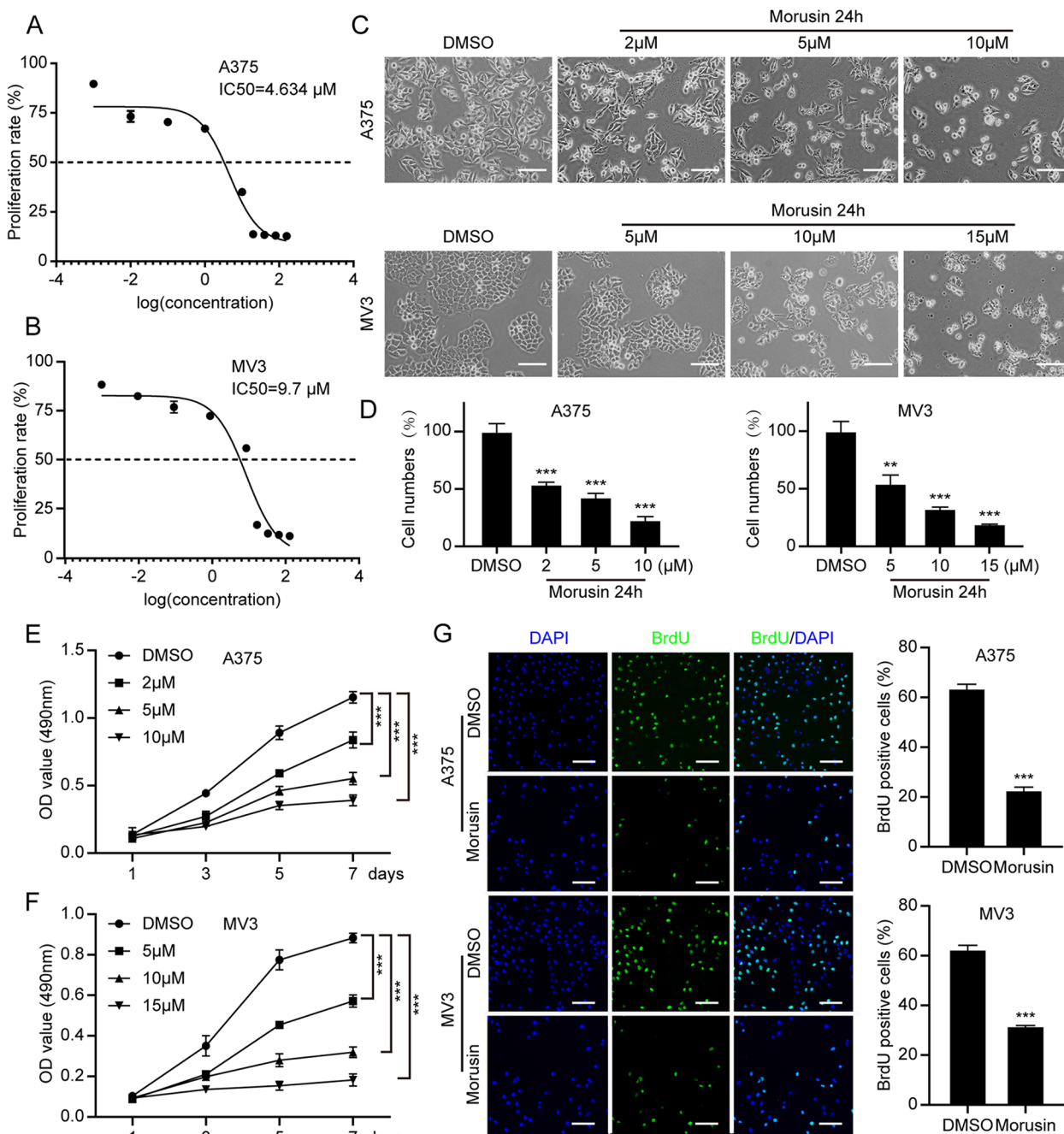


Fig. 1 Morusin inhibits cell growth and proliferation in melanoma cells. The IC₅₀ of **A** A375 and **B** MV3 cells. **C** The cell morphology of A375 and MV3 cells after treating with indicated concentration of morusin for 24 h. DMSO was used as control. Scale bar was 100 μm. **D** The cell numbers of A375 and MV3 were counted and displayed. The DMSO treatment group was considered to be 100%. The viability of **E** A375 and **F** MV3 after treating with DMSO or morusin. **G** The image and quantification of BrdU staining cells of A375 and MV3 after treating with DMSO or morusin (5 μM for A375 and 10 μM for MV3) for 24 h. Scale bar was 100 μm. Each experiment was repeated three times. All data were shown as the mean ± SD and analyzed by two-tailed Student's t-test. **P* < 0.05, ***P* < 0.01, ****P* < 0.001

the US FDA for the treatment of melanoma, and its therapeutic effect is obvious. In this experiment, we examined the change in cell viability after 24 h treatment of A375 and MV3 cells with different concentrations of DTIC

(CAS: 4342-03-4; Shanghai, China), and the results showed that the IC₅₀ of A375 cells was 81.9 μM (Fig. S1J) and the IC₅₀ of MV3 cells was 84.7 μM (Fig. S1K). In the MTT experiment, we can see that the growth curve

of A375 cells decrease more slowly after 5 μM morusin treatment than after 80 μM DTIC treatment (Fig. S1L). Similarly, the same results can be obtained after 10 μM morusin treatment and 85 μM DTIC treatment of MV3 cells (Fig. S1M). BrdU staining assay showed that morusin remarkably decreased the percentage of BrdU-positive cells, compared with DMSO-treated cells in A375 and MV3 (Fig. 1G). These results suggested that morusin had a significant inhibitory effect on the cell proliferation in melanoma cells.

Morusin induces cell cycle arrest at G2/M phase in melanoma cells

Cell proliferation is closely related to the cell cycle. Next, we further explored whether morusin has effect on the cell cycle. The cell cycle was detected by PI single-staining flow cytometry. The results showed that comparing with the control group, the percentage of G2/M phase cells was significantly increased after treating with 2 and 5 μM morusin on A375 cells, 5 and 10 μM morusin on MV3 cells for 24 h. The difference was statistically significant ($P < 0.05$) (Fig. 2A and B). Western blot experiment further verified the expression levels of related cyclins. The results showed that, after treatment with morusin, the protein expression levels of p53 and p21 were increased in a concentration-dependent manner (A375 cells were treated with DMSO, 2 μM , 5 μM , 10 μM , and the doses treated on MV3 cells were DMSO, 5 μM , 10 μM , 15 μM) and time-dependent manner (0 h, 12 h, 24 h, 36 h). In the meantime, CyclinB1 and CDK1 was down-regulated (Fig. 2C-F). Above results indicated that morusin induces cell cycle arrest at G2/M phase, thereby inhibiting the proliferation of melanoma cells.

Morusin induces apoptosis in melanoma cells

In order to explore whether morusin can also induce apoptosis, we used AnnexinV-APC and PI for flow cytometry assay. As shown in Fig. 3A and B, there was obvious apoptosis after morusin treatment. To further certify this result, we treated A375 cells with 0, 2, 5 and 10 μM , MV3 cells with 0, 5, 10 and 15 μM morusin for 24 h. Western blot assay results showed that Cleaved-PARP (C-PARP) and Cleaved-Caspase3 (C-Caspase3) increased in a dose-dependent manner (Fig. 3C and D). Besides, we also found that the levels of C-PARP and

C-Caspase3 were increased in a time-dependent manner (Fig. 3E and F). All the results suggested that morusin induces apoptosis in melanoma cells.

Morusin inhibits cell migration and invasion in melanoma cells

Melanoma cells have the superior ability of migration and invasion. In order to explore the effect of morusin on the migration and invasion ability of melanoma cells, we conducted wound healing assay, transwell migration and invasion assays and Western blot experiment. Wound healing assay showed that melanoma cells treated with morusin had a significantly weaker ability to heal scratches than the control group (Fig. 4A and B). Transwell migration assay also revealed that the migration ability of the melanoma cells treated with morusin was significantly reduced comparing with the control group (Fig. 4C). Similarly, the result of invasion assay showed that the number of cells crossed the matrigel was significantly reduced after morusin-treated comparing with control group (Fig. 4D). Western blot assay indicated that morusin up-regulated E-Cadherin and down-regulated Vimentin expression in a dose-dependent and time-dependent manner (Fig. 4E-H). And we found that the expression of MMP2 was also down-regulated with the concentration and time of morusin (Fig. S1G and H). To sum up, these findings demonstrated that morusin inhibits cell migration and invasion in melanoma cells.

Morusin inhibits tumor growth both in vitro and in vivo

To further assess the effects of morusin in colony formation, we used the melanoma A375 and MV3 cells as the research objects to conduct soft agar clone formation experiment. The inverted microscope showed that comparing with the control group, the size of single clone in the morusin treatment groups was significantly smaller, and the number of clones formed was significantly reduced (Fig. 5A and B). Next, MV3 cells were injected subcutaneously into four-week-old mice, and the growth status of the mice were observed every two days. It was observed that there was no significant difference between the body weights of the experimental group and the control group (Fig. 5C). The tumor volume of the morusin treatment group was lower than the control group (Fig. 5D). And the tumor weight and size of the morusin

(See figure on next page.)

Fig. 2 Morusin induces cell cycle arrest at G2/M phase in melanoma cells. **A** The cell cycle of A375 and MV3 cells treated with DMSO or morusin (5 μM for A375 and 10 μM for MV3) for 24 h was analyzed by flow cytometry. **B** Percentage of indicated A375 and MV3 cells in different periods. **C** The expression levels of CyclinB1, p53, p21 and CDK1 in A375 and MV3 cells treated with morusin in different concentrations (2, 5, 10 μM for A375 and 5, 10, 15 μM for MV3) or DMSO for 24 h were determined by Western blot analysis. Tubulin was used as a control. **D** Densitometry of western blot in panel C. **E** The expression levels of CyclinB1, p53, p21 and CDK1 in A375 and MV3 cells treated with morusin (5 μM for A375 and 10 μM for MV3) in different times for 0, 12, 24, 36 h. Tubulin was used as a control. **F** Densitometry of western blot in panel E. Each experiment was repeated three times. All data were shown as the mean \pm SD and analyzed by two-tailed Student's t-test. * $P < 0.05$, ** $P < 0.01$, *** $P < 0.001$

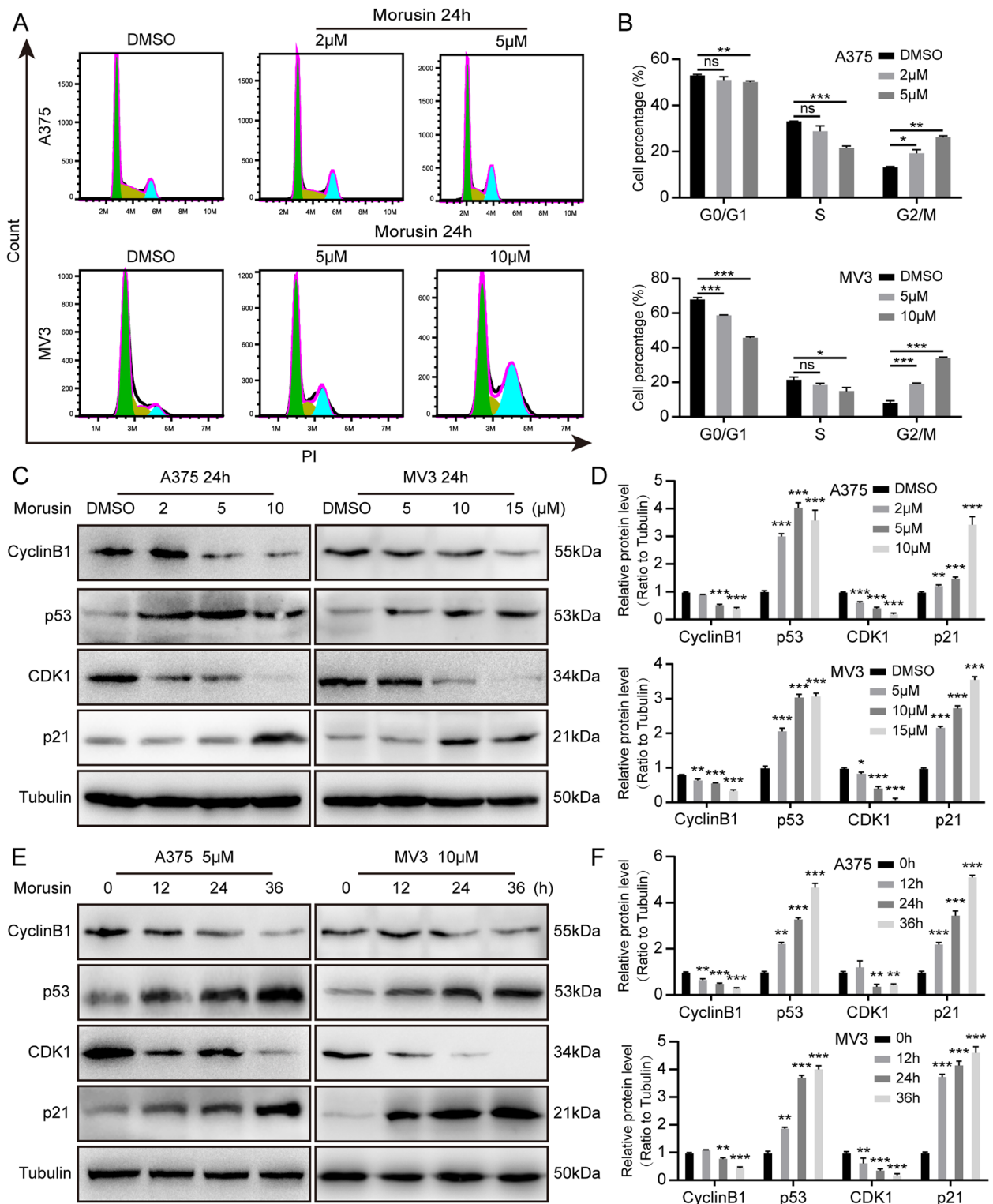


Fig. 2 (See legend on previous page.)

treatment group were obviously smaller than the control group (Fig. 5E and F). At the same time, the hematoxylin–eosin (H&E) results showed that comparing with the control group, the number of cells in the experimental group was reduced and the nucleus became smaller, and the immunohistochemistry (IHC) staining results suggested that the expressions of Ki67, CDK1 and CyclinB1 were significantly reduced, while the expressions of p53 and p21 were increased in the morusin-treated group (Fig. 5G and H) (Fig. S1N). The data indicated morusin could inhibit the colonization of melanoma cells and inhibit tumor formation in mice.

Morusin-inducing cell proliferation inhibition, cell cycle arrest, apoptosis, and metastasis can be partially recovered by knocking down the p53

As is known to all, p53 as a tumor suppressor can maintain normal development and tissue homeostasis [36]. Meanwhile, we found that the expression of p53 was remarkably increased in A375 and MV3 after treatment with morusin. Therefore, the expression of p53 in A375 and MV3 cells was detected by qRT-PCR. The results showed that morusin increased the mRNA expression of p53 (Fig. S1B). In order to explore the role of p53 in our experiment, we successfully knocked down p53 in A375 cells (Fig. 6A). MTT assay showed that after treating with 5 μ M morusin in A375 cells, the cell growth was partially recovered by knocking down p53 (Fig. 6B). At the same time, BrdU staining results indicated that knock down p53 could rescue the DNA synthesis reduced by morusin (Fig. 6C). To investigate whether knock down of p53 effect the cell cycle, we treated the shGFP and shp53 group with 5 μ M morusin and then performed with flow cytometry analysis. The results showed that the percentage of G2/M phase in the shp53 group showed a slight decrease after treating with morusin for 24 h in A375 cells (Fig. 6D), which means knocking down p53 could rescue cell cycle arrest induced by morusin. Subsequently, we examined the effect on apoptosis. A375 cells were treated with 5 μ M morusin for shp53 group and shGFP group. After 24 h, flow cytometry showed that comparing with the shGFP group, the shp53 group showed a decline in cells apoptosis (Fig. 6E), which indicated that knocking down p53 could alleviate apoptosis induced by morusin. In addition, the migration and

invasion assay found that the number of cell migration and invasion increased in the shp53 group comparing with the shGFP group (Fig. 6F), suggesting that knocking down p53 could rescue the reduced ability of cell migration and invasion induced by morusin. Finally, Western blot results also showed that comparing with the shGFP group, the expression levels of p53, p21, C-Caspase3 and E-Cadherin were decreased (Fig. 6G), and the expression levels of CDK1 and CyclinB1 were increased (Fig. S1I) in shp53 group following morusin treatment. The above results indicated that morusin-inducing cell proliferation inhibition, cell cycle arrest, apoptosis, and metastasis could be partially recovered by knocking down p53.

Discussion

Melanoma, a malignant tumor of the skin, is caused by the excessive proliferation of melanocytes, and its incidence is increasing [37]. Surgery combined with chemotherapy is the main treatment, but due to the strong invasion and metastasis ability of melanoma cells, the current treatment cannot achieve satisfactory therapeutic effect [38, 39]. Therefore, it is particularly important to explore new and efficient treatment methods.

Flavonoids, a kind of natural products, are widely found in the plant kingdom. They not only have anti-inflammatory, antioxidant, antiviral and neuroprotective effects [40], but also have a killing effect on tumor cells. Morusin is one of the important flavonoids. Recent studies showed that morusin had anti-cancer activity in many human cancers, such as breast cancer [41], pancreatic cancer [42], lung cancer [43, 44] and other tumor types [21, 22, 45]. In addition, Morusin ameliorates IL-1 β -Induced chondrocyte inflammation and osteoarthritis via NF- κ B signal pathway [46]. Meanwhile, as an anticancer candidate, morusin exerts antitumor effects in hepatocellular cancers through AMPK-mediated G1 arrest and anti-glycolysis [47]. Still, the anti-tumor activity of morusin in human melanoma is unclear. In this study, we found, for the first time, that morusin has anti-melanoma effect. We used different concentrations of morusin to treat human melanoma cells A375 and MV3. The MTT assays indicated that morusin inhibits cell proliferation in a dose-dependent and time-dependent manner. Additionally, we found that the IC₅₀ of morusin is significantly high in the normal PIG1 and HaCaT cells, then treating PIG1

(See figure on next page.)

Fig. 3 Morusin induces apoptosis in melanoma cells. **A** Apoptosis of A375 and MV3 cells treated with DMSO or morusin (2, 5 μ M for A375 and 5, 10 μ M for MV3) for 24 h was analyzed by flow cytometry. **B** Apoptosis rate of melanoma cells in Panel A. **C** The expression levels of PARP and Caspase3 in A375 and MV3 cells treated with morusin in different concentrations (2, 5, 10 μ M for A375 and 5, 10, 15 μ M for MV3) or DMSO for 24 h were determined by Western blot analysis. Tubulin was used as a control. **D** Densitometry of western blot in panel C. **E** The expression levels of PARP and Caspase3 in A375 and MV3 cells treated with morusin (5 μ M for A375 and 10 μ M for MV3) in different times for 0, 12, 24, 36 h. Tubulin was used as a control. **F** Densitometry of western blot in panel E. Each experiment was repeated three times. All data were shown as the mean \pm SD and analyzed by two-tailed Student's t-test. * P < 0.05, ** P < 0.01, *** P < 0.001

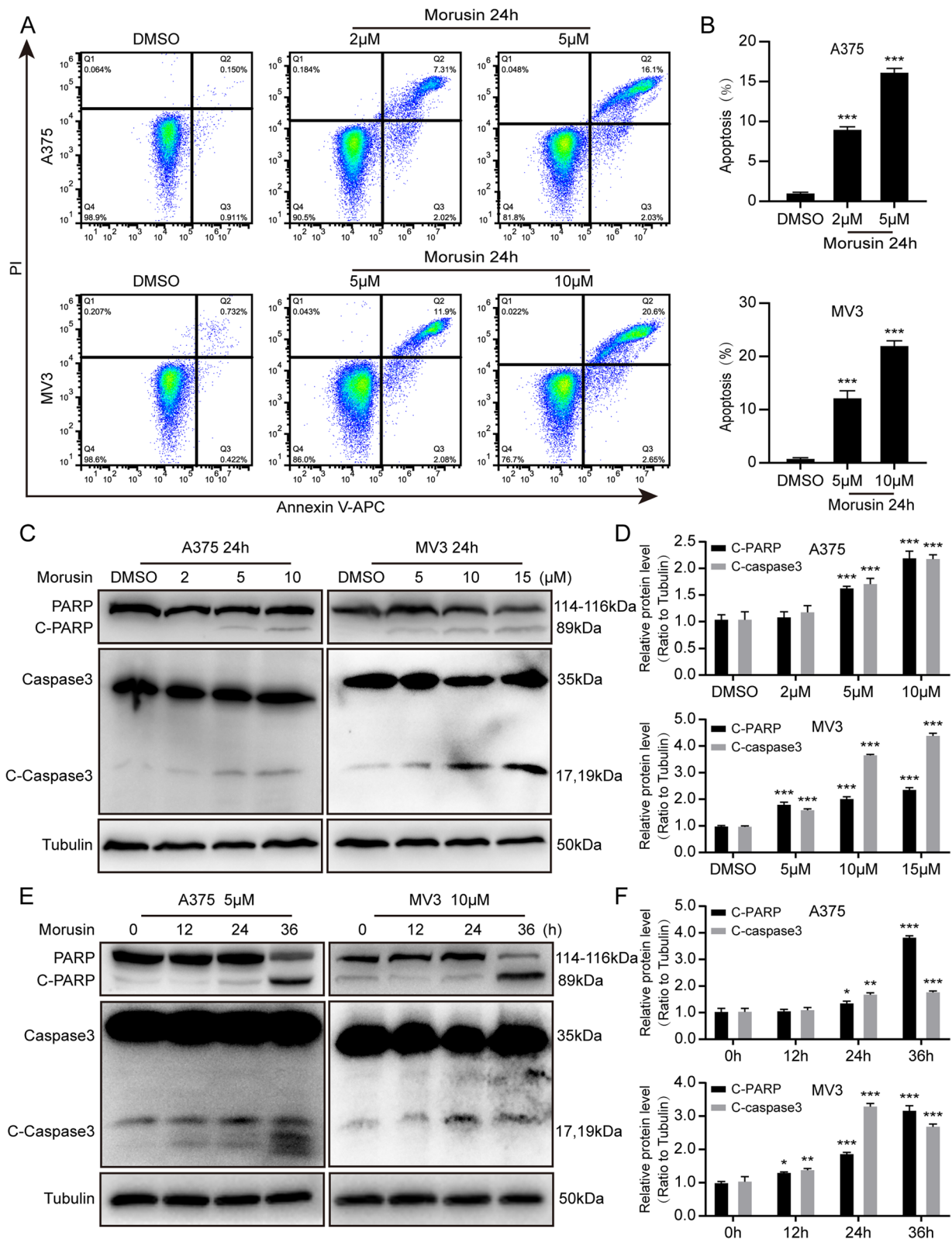


Fig. 3 (See legend on previous page.)

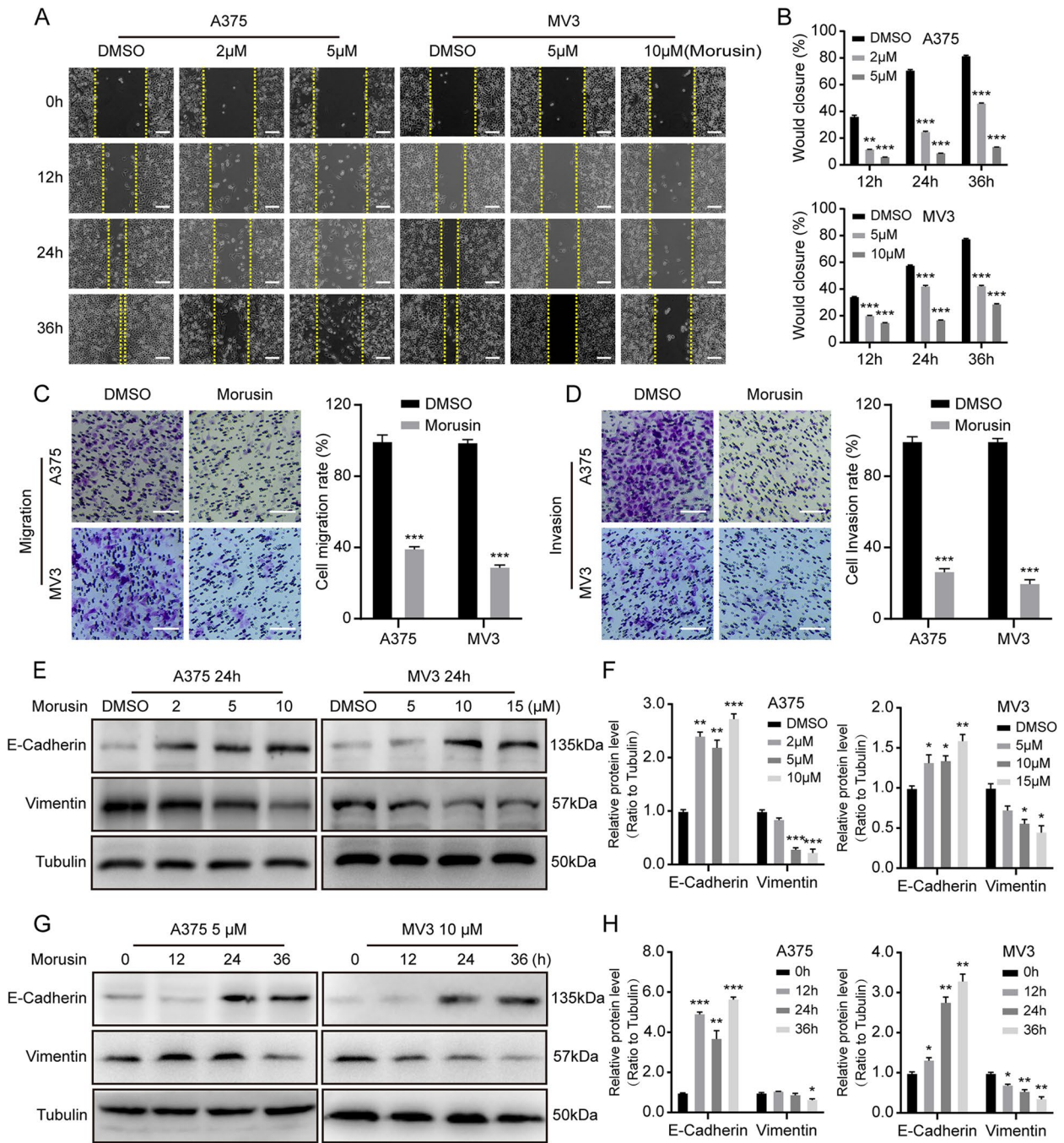


Fig. 4 Morusin inhibits cell migration and invasion in melanoma cells. **A** The migration of A375 and MV3 cells treated with morusin for the corresponding time was measured by wound-healing assay. Scale bar was 100 μ m. **B** The effect of morusin on the healing of melanoma cells. The healing rate of 0 h was considered to be 100%. **C** Transwell migration assays of A375 and MV3 cells treated with DMSO or morusin (5 μ M for A375 and 10 μ M for MV3) for 24 h. Scale bar was 100 μ m. The statistical analysis was presented in histograms, and cell migration rates were normalized by proliferation. **D** Transwell invasion assays of A375 and MV3 cells treated with DMSO or morusin (5 μ M for A375 and 10 μ M for MV3) for 72 h. Scale bar was 100 μ m. Cell invasion rates were normalized by proliferation. **E** The expression levels of E-Cadherin and Vimentin in A375 and MV3 cells treated with morusin in different concentrations (2, 5, 10 μ M for A375 and 5, 10, 15 μ M for MV3) or DMSO for 24 h. **F** Densitometry of western blot in panel E. **G** The expression levels of E-Cadherin and Vimentin in A375 and MV3 cells treated with morusin (5 μ M for A375 and 10 μ M for MV3) in different times for 0, 12, 24, 36 h. Tubulin was used as the control. **H** Densitometry of Western blot in panel G. Each experiment was repeated three times. All data were shown as the mean \pm SD and analyzed by two-tailed Student's t-test. * P < 0.05, ** P < 0.01, *** P < 0.001

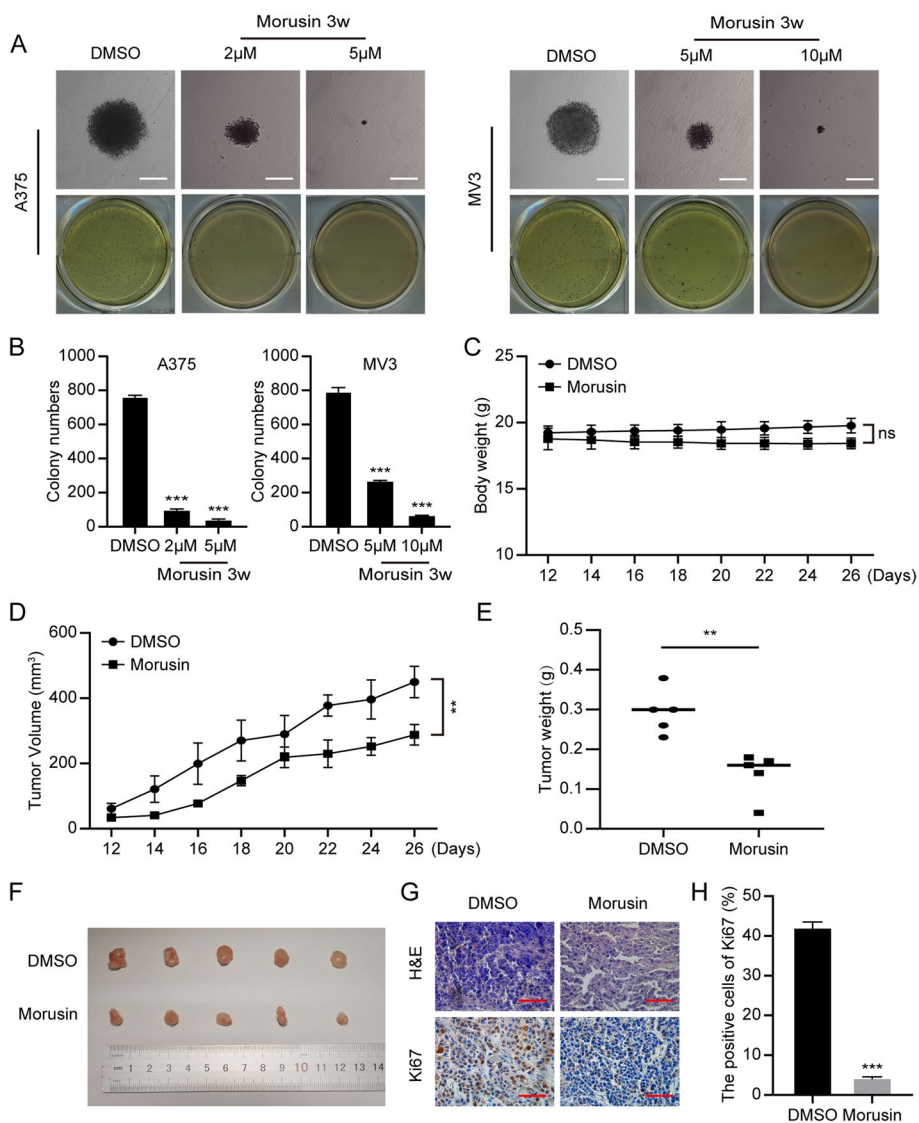


Fig. 5 Morusin inhibits tumor growth in vitro and in vivo. **A** The clone formation ability of A375 and MV3 after treating with 5 and 10 µM morusin was detected by soft agar assay. Scale bar was 100 µm. **B** Colony numbers in panel A were quantified. **C** Body weight of mice treated with morusin or DMSO. **D** Tumor volume of mice treated with morusin (25 mg/kg) or DMSO. **E** Tumor weight of mice treated with morusin (25 mg/kg) or DMSO. **F** Photograph of tumors from indicated mice. **G** H&E and IHC staining of Ki67 in indicated tumors. Scale bar was 100 µm. **H** The positive cells of Ki67 in panel G. All data were shown as the mean ± SD and analyzed by two-tailed Student’s t-test. **P* < 0.05, ***P* < 0.01, ****P* < 0.001

(See figure on next page.)

Fig. 6 Morusin-inducing cell proliferation inhibition, cell cycle arrest, apoptosis, and metastasis can be recovered by knocking down p53. **A** The expression level of p53 was detected by Western blot in A375 cells. **B** Growth curve of knock down p53 after treating with 5 µM morusin in A375 cells. DMSO and shGFP were used as control. **C** The image and quantification of BrdU positive cells in knockdown p53 A375 cells treatment with 5 µM morusin for 24 h. Scale bar was 100 µm. **D** Cell cycle was detected in knockdown p53 A375 cells after treating with 5 µM morusin for 24 h, and percentage of A375 cells in different phase. DMSO and shGFP were used as control. **E** Apoptosis of knockdown p53 A375 cells treated with 5 µM morusin for 24 h was analyzed by flow cytometry, and apoptosis rate of melanoma cells was quantified. DMSO and shGFP were used as control. **F** Transwell migration and invasion assays of knockdown p53 A375 cells treated with 5 µM morusin for 24 h and 72 h were analysed. Scale bar was 100 µm. DMSO and shGFP were used as control. Cell migration and invasion rates were normalized. **G** The expression of p53, p21, C-Caspase3 and E-Cadherin were checked in knockdown p53 A375 cells treated with 5 µM morusin for 24 h. DMSO and shGFP were used as control. Tubulin was used as the control. All data were shown as the mean ± SD and analyzed by two-tailed Student’s t-test. **P* < 0.05, ***P* < 0.01, ****P* < 0.001

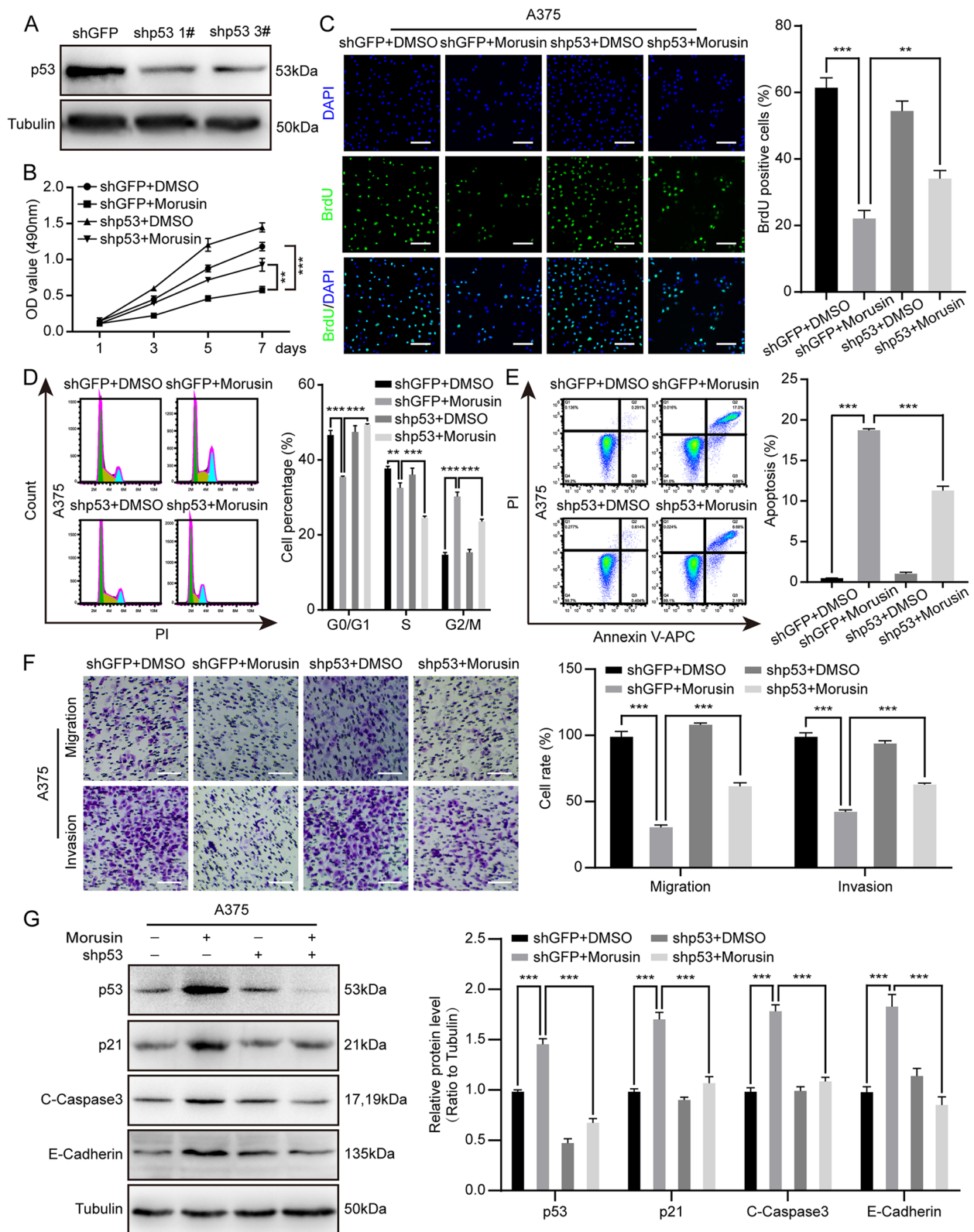


Fig. 6 (See legend on previous page.)

and HaCaT with IC₅₀ of morusin in MV3 (10 μM), which is the highest concentration used in cancer cells in this study, showed no obvious toxicity. Dacarbazine (DTIC) is the first generation of drugs approved by the US FDA for the treatment of melanoma, and its therapeutic effect is obvious, and many scholars have studied the efficacy of dacarbazine [48, 49]. In our experiments, we can see that 80 μM DTIC has a significant inhibitory effect on the growth of A375 cells. At the same time, 5 μM morusin has a better inhibitory effect on A375 cells. The same result was found in MV3 cells. Of course, this result needs to be verified in the clinic in the future. BrdU assays also showed a remarkable decrease in the percentage of BrdU-positive cells which were treated with morusin. The soft agar assays suggested that after treatment with morusin, the colonies were lesser and smaller than the DMSO group. In vivo, xenograft experiment showed that the tumor volume and weight were significant reduced. All evidence above indicated that morusin could inhibit the growth of melanoma cells in vitro and in vivo.

Cell proliferation is usually associated with the cell cycle. Current studies have shown that cell cycle can be blocked in the G₀/G₁ phase after treatment with morusin [24, 50]. Morusin could inhibit three RCC cell lines, 769-P, 786-O, and OSRC-2 cell, growth and migration, and disturb the cell cycle arrest in the G₁ phase [24]. As we all know, the *p53* is the most common transcription factor in many human cancers. It plays an important role in the metabolism of normal cells and cancer cells, and it is often lost in cancer [51, 52]. In our study, cell cycle analysis showed that morusin inhibits the cell cycle in the G₂/M phase by down-regulating CyclinB1 and CDK1, and up-regulating *p53* and *p21*. Therefore, we guessed that morusin blocked the cell cycle in the G₂/M phase through the *p53/p21* axis. Previous reports have shown that morusin can induce apoptosis of a variety of cancer cells [44, 45, 53–56]. For example, morusin can induce apoptosis of pancreatic tumor cells and loss of mitochondrial membrane potential [42]. Based on these results, we performed apoptosis assay and Western blot to explore the effect of morusin on melanoma cells. The main findings in these studies are that morusin promotes apoptosis of melanoma cells by up-regulating C-PARP and C-Caspase3. Furthermore, because melanoma is prone to metastasis and has a strong ability of invasion [57–59], and studies have shown that after mulberry treatment of kidney cancer cells [24], lung cancer cells [43], cell migration ability is significantly limited, we proved that morusin could significantly inhibit the migration and invasion ability of melanoma cells. These studies suggest that morusin can not only induce cell cycle arrest and induce apoptosis, but also inhibit the migration and invasion ability

of melanoma cells. Similarly, in mouse experiments, we also confirmed that morusin can inhibit tumorigenesis in mice. When selecting a mouse tumor model, we subcutaneously injected human melanoma cells into NOD/SCID immunodeficient mice, which are highly homologous, but the tumor heterogeneity may be slightly less than that in the syngeneic transplant mouse model.

Immune checkpoint inhibitor (ICI)-mediated immunotherapy can interfere with tumor and immune system functions by affecting multiple immune pathways [60]. Although immune-related adverse events may occur [61], its clinical efficacy and safety are worthy of recognition [62]. Immunotherapy mediated by it is a new direction of anti-tumor therapy for various cancers in recent years [63, 64]. As an important target for cancer therapy [65], *p53* has been found to regulate IFN-γ-stimulated PD-L1 expression in melanoma [66]. In addition, clinical studies have found that the use of immunosuppressive agents can provide more durable survival benefits for patients with advanced melanoma [67, 68]. When DNA damage or stress occurs, *p53* levels will increase, and it can induce cell cycle arrest and apoptosis [69–72]. In addition, no mutation of *p53* gene in human melanoma A375-S2, A375-C6 cells has been reported [73, 74]. In order to further explore the role of *p53* in our experiment, we successfully knocked down the *p53* in A375 cells. We found that comparing with shGFP, knocking down *p53* can partly rescue the cell growth inhibition, cell cycle arrest, apoptosis and the decreased ability of migration and invasion caused by morusin. Therefore, our results indicate that knocking down *p53* can rescue the changes in proliferation, apoptosis and metastasis caused by morusin. Therefore, we suggest that morusin increases the expression of *p53*, which is a good strategy for the treatment of melanoma.

Conclusion

Collectively, this study demonstrates that morusin can inhibit proliferation, migration, invasion, and survival of melanoma cells, through activating *p53*-mediated pathways, therefore providing a theoretical basis for morusin to be a potential drug for the treatment of melanoma in the future.

Supplementary Information

The online version contains supplementary material available at <https://doi.org/10.1186/s12885-023-11080-1>.

Additional file 1.

Additional file 2.

Additional file 3.

Acknowledgements

We sincerely thank Lichao Liu, Yanli Zhang, Huanrong Hu, Xiaosong Hu, Guangzhao Pan, Guanghui Zhang, and Yongsen Li for their technical support and helpful suggestions for this experiment. We are very grateful to the State Key Laboratory of Silkworm Genome Biology, Southwest University.

Authors' contributions

WL, YCJ and FW designed the experiments. All authors performed the experiments. WL wrote the original manuscript. CYL, SMS, RCL and QL provided reagents and technical assistance. YCJ and LYG conducted the data collection and statistical analysis. YLL and HJC funded and supervised the project, and modified the manuscript. All authors are in agree with the content of the manuscript.

Funding

This research was supported by the National Natural Science Foundation of China (81872071), the Natural Science Foundation of Chongqing (cstc2019jcyj-zdxmX0033), the Fundamental Research Funds for the Central Universities (XYDS201912) and Chongqing University Innovation Team Building Program funded projects (CXTDX201601010).

Availability of data and materials

The datasets used and/or analyzed during the current study are available from the corresponding author on reasonable request.

Declarations

Ethics approval and consent to participate

All animal experiments were approved by the animal ethics committee of Southwest University. And all methods were performed in accordance with the relevant guidelines and regulations of the Basel Declaration. And the study is reported in accordance with ARRIVE guidelines.

Consent for publication

Not applicable.

Competing interests

Wei Liu, Yacong Ji, Feng Wang, Chongyang Li, Shaomin Shi, Ruochen Liu, Qian Li, Leyang Guo, Yaling Liu and Hongjuan Cui declare no competing interests.

Author details

¹Department of Dermatology, The Third Hospital of Hebei Medical University, Ziqiang Road 139, 050000 Shijiazhuang, China. ²State Key Laboratory of Silkworm Genome Biology, Southwest University, No. 2 Tiansheng Road, Beibei District, 400715 Chongqing, P.R. China. ³Cancer Centre, Reproductive Medicine Centre, Medical Research Institute, Southwest University, Chongqing, China. ⁴Department of Pathology, School of Basic Medical Sciences, Fudan University, Shanghai, China. ⁵The Ninth People's Hospital of Chongqing, Affiliated Hospital of Southwest University, Chongqing, China.

Received: 22 November 2022 Accepted: 16 June 2023

Published online: 29 June 2023

References

- Siegel RL, Miller KD, Jemal A. Cancer statistics, 2020. *CA Cancer J Clin*. 2020;70(1):7–30.
- Morton DL, Thompson JF, Cochran AJ, Mozzillo N, Elashoff R, Essner R, Nieweg OE, Roses DF, Hoekstra HJ, Karakousis CP, et al. Sentinel-node biopsy or nodal observation in melanoma. *N Engl J Med*. 2006;355(13):1307–17.
- Falk Delgado A, Zommorodi S, Falk Delgado A. Sentinel Lymph Node Biopsy and Complete Lymph Node Dissection for Melanoma. *Curr Oncol Rep*. 2019;21(6):54.
- Tas F, Erturk K. Recurrence behavior in early-stage cutaneous melanoma: pattern, timing, survival, and influencing factors. *Melanoma Res*. 2017;27(2):134–9.
- Garbe C, Peris K, Hauschild A, Saiag P, Middleton M, Spatz A, Grob JJ, Malvehy J, Newton-Bishop J, Stratigos A, et al. Diagnosis and treatment of melanoma: European consensus-based interdisciplinary guideline. *Eur J Cancer*. 2010;46(2):270–83.
- Fontana F, Raimondi M, Di Domizio A, Moretti RM, Montagnani Marelli M, Limonta P. Unraveling the molecular mechanisms and the potential chemopreventive/therapeutic properties of natural compounds in melanoma. *Semin Cancer Biol*. 2019;59:266–82.
- Albuquerque KRS, Pacheco NM, Del Rosario Loyo Casao T, de Melo F, Novaes RD, Gonçalves RV. Applicability of Plant Extracts in Preclinical Studies of Melanoma: A Systematic Review. *Mediators Inflamm*. 2018;2018:6797924.
- Imran M, Rauf A, Abu-Izneid T, Nadeem M, Shariati MA, Khan IA, Imran A, Orhan IE, Rizwan M, Atif M, et al. Luteolin, a flavonoid, as an anticancer agent: A review. *Biomed Pharmacother*. 2019;112: 108612.
- Gadotti VM, Zamponi GW. Anxiolytic effects of the flavonoid luteolin in a mouse model of acute colitis. *Mol Brain*. 2019;12(1):114.
- Nabavi SF, Braidy N, Gortzi O, Sobarzo-Sanchez E, Daglia M, Skalicka-Woźniak K, Nabavi SM. Luteolin as an anti-inflammatory and neuroprotective agent: A brief review. *Brain Res Bull*. 2015;119(Pt A):1–11.
- Schomberg J, Wang Z, Farhat A, Guo KL, Xie J, Zhou Z, Liu J, Kovacs B, Liu-Smith F. Luteolin inhibits melanoma growth in vitro and in vivo via regulating ECM and oncogenic pathways but not ROS. *Biochem Pharmacol*. 2020;177: 114025.
- Yao X, Jiang W, Yu D, Yan Z. Luteolin inhibits proliferation and induces apoptosis of human melanoma cells in vivo and in vitro by suppressing MMP-2 and MMP-9 through the PI3K/AKT pathway. *Food Funct*. 2019;10(2):703–12.
- Li C, Wang Q, Shen S, Wei X, Li G. HIF-1 α /VEGF signaling-mediated epithelial-mesenchymal transition and angiogenesis is critically involved in anti-metastasis effect of luteolin in melanoma cells. *Phytotherapy research* : PTR. 2019;33(3):798–807.
- Pourhanifeh MH, Abbaszadeh-Goudarzi K, Goodarzi M, Piccirillo SGM, Shafiee A, Hajighadimi S, Moradizarmehri S, Asemi Z, Mirzaei H. Resveratrol: A new potential therapeutic agent for melanoma? *Curr Med Chem*. 2019.
- Mokhamatam RB, Sahoo BK, Manna SK. Suppression of microphthalmia-associated transcription factor, but not NF- κ B sensitizes melanoma specific cell death. *Apoptosis*. 2016;21(8):928–40.
- Zhao H, Han L, Jian Y, Ma Y, Yan W, Chen X, Xu H, Li L. Resveratrol induces apoptosis in human melanoma cell through negatively regulating Erk/PKM2/Bcl-2 axis. *Oncotargets Ther*. 2018;11:8995–9006.
- Saha B, Pai GB, Subramanian M, Gupta P, Tyagi M, Patro BS, Chattopadhyay S. Resveratrol analogue, trans-4,4'-dihydroxystilbene (DHS), inhibits melanoma tumor growth and suppresses its metastatic colonization in lungs. *Biomed Pharmacother*. 2018;107:1104–14.
- Carletto B, Berton J, Ferreira TN, Dalmolin LF, Paludo KS, Mainardes RM, Farago PV, Favero GM. Resveratrol-loaded nanocapsules inhibit murine melanoma tumor growth. *Colloids Surf B Biointerfaces*. 2016;144:65–72.
- Imenshahidi M, Hosseinzadeh H. Berberis Vulgaris and Berberine: An Update Review. *Phytother Res*. 2016;30(11):1745–64.
- Liu JF, Lai KC, Peng SF, Maraming P, Huang YP, Huang AC, Chueh FS, Huang WW, Chung JG. Berberine Inhibits Human Melanoma A375.S2 Cell Migration and Invasion via Affecting the FAK, uPA, and NF- κ B Signaling Pathways and Inhibits PLX4032 Resistant A375.S2 Cell Migration In Vitro. *Molecules* 2018, 23(8).
- Wang F, Zhang D, Mao J, Ke XX, Zhang R, Yin C, Gao N, Cui H. Morusin inhibits cell proliferation and tumor growth by down-regulating c-Myc in human gastric cancer. *Oncotarget*. 2017;8(34):57187–200.
- Cho SW, Na W, Choi M, Kang SJ, Lee SG, Choi CY. Autophagy inhibits cell death induced by the anti-cancer drug morusin. *Am J Cancer Res*. 2017;7(3):518–30.
- Lee JC, Won SJ, Chao CL, Wu FL, Liu HS, Ling P, Lin CN, Su CL. Morusin induces apoptosis and suppresses NF- κ B activity in human colorectal cancer HT-29 cells. *Biochem Biophys Res Commun*. 2008;372(1):236–42.
- Yang C, Luo J, Luo X, Jia W, Fang Z, Yi S, Li L. Morusin exerts anti-cancer activity in renal cell carcinoma by disturbing MAPK signaling pathways. *Annals of translational medicine*. 2020;8(6):327.
- Park HJ, Min TR, Chi GY, Choi YH, Park SH. Induction of apoptosis by morusin in human non-small cell lung cancer cells by suppression of EGFR/STAT3 activation. *Biochem Biophys Res Commun*. 2018;505(1):194–200.

26. Gao L, Wang L, Sun Z, Li H, Wang Q, Yi C, Wang X. Morusin shows potent antitumor activity for human hepatocellular carcinoma in vitro and in vivo through apoptosis induction and angiogenesis inhibition. *Drug Des Devel Ther.* 2017;11:1789–802.
27. Oikawa T, Okuda M, Ma Z, Goorha R, Tsujimoto H, Inokuma H, Fukasawa K. Transcriptional control of BubR1 by p53 and suppression of centrosome amplification by BubR1. *Mol Cell Biol.* 2005;25(10):4046–61.
28. Wu Q, Zhang KJ, Jiang SM, Fu L, Shi Y, Tan RB, Cui J, Zhou Y. p53: A Key Protein That Regulates Pulmonary Fibrosis. *Oxid Med Cell Longev.* 2020;2020:6635794.
29. Lee YK, Chung Y, Lee JH, Chun JM, Park JH. The Intricate Role of p53 in Adipocyte Differentiation and Function. *Cells.* 2020;9(12).
30. Li C, Deng C, Pan G, Wang X, Zhang K, Dong Z, Zhao G, Tan M, Hu X, Shi S, et al. Lycorine hydrochloride inhibits cell proliferation and induces apoptosis through promoting FBXW7-MCL1 axis in gastric cancer. *J Exp Clin Cancer Res.* 2020;39(1):230.
31. Zhao Y, He J, Li J, Peng X, Wang X, Dong Z, Zhao E, Liu Y, Wu Z, Cui H. Demethylzeylasteral inhibits cell proliferation and induces apoptosis through suppressing MCL1 in melanoma cells. *Cell Death Dis.* 2017;8(10):e3133.
32. Du J, Dong Z, Tan L, Tan M, Zhang F, Zhang K, Pan G, Li C, Shi S, Zhang Y, et al. Tubeimoside I Inhibits Cell Proliferation and Induces a Partly Disrupted and Cytoprotective Autophagy Through Rapidly Hyperactivation of MEK1/2-ERK1/2 Cascade via Promoting PTP1B in Melanoma. *Front Cell Dev Biol.* 2020;8: 607757.
33. Ke XX, Zhang R, Zhong X, Zhang L, Cui H. Deficiency of G9a Inhibits Cell Proliferation and Activates Autophagy via Transcriptionally Regulating c-Myc Expression in Glioblastoma. *Front Cell Dev Biol.* 2020;8: 593964.
34. Hu H, Dong Z, Tan P, Zhang Y, Liu L, Yang L, Liu Y, Cui H. Antibiotic drug tigecycline inhibits melanoma progression and metastasis in a p21CIP1/Waf1-dependent manner. *Oncotarget.* 2016;7(3):3171–85.
35. Shi S, Li C, Zhang Y, Deng C, Liu W, Du J, Li Q, Ji Y, Guo L, Liu L, et al. Dihydrocapsaicin Inhibits Cell Proliferation and Metastasis in Melanoma via Down-regulating β -Catenin Pathway. *Front Oncol.* 2021;11: 648052.
36. Ghatak D, Das Ghosh D, Roychoudhury S. Cancer Stemness: p53 at the Wheel. *Front Oncol.* 2020;10: 604124.
37. Costantino VV, Lobos-Gonzalez L, Ibañez J, Fernandez D, Cuello-Carrión FD, Valenzuela MA, Barbieri MA, Semino SN, Jahn GA, Quest AF, et al. Dehydroleucodine inhibits tumor growth in a preclinical melanoma model by inducing cell cycle arrest, senescence and apoptosis. *Cancer Lett.* 2016;372(1):10–23.
38. Mishra H, Mishra PK, Ekielski A, Jaggi M, Iqbal Z, Talegaonkar S. Melanoma treatment: from conventional to nanotechnology. *J Cancer Res Clin Oncol.* 2018;144(12):2283–302.
39. Kawaguchi K, Igarashi K, Murakami T, Chmielowski B, Kiyuna T, Zhao M, Zhang Y, Singh A, Unno M, Nelson SD, et al. Tumor-targeting Salmonella typhimurium A1-R combined with temozolomide regresses malignant melanoma with a BRAF-V600E mutation in a patient-derived orthotopic xenograft (PDOX) model. *Oncotarget.* 2016;7(52):85929–36.
40. Panek-Krzyśko A, Stompor-Gorący M. The Pro-Health Benefits of Morusin Administration-An Update Review. *Nutrients.* 2021;13(9).
41. Kang S, Kim EO, Kim SH, Lee JH, Ahn KS, Yun M, Lee SG. Morusin induces apoptosis by regulating expression of Bax and Survivin in human breast cancer cells. *Oncol Lett.* 2017;13(6):4558–62.
42. Kim C, Kim JH, Oh EY, Nam D, Lee SG, Lee J, Kim SH, Shim BS, Ahn KS. Blockage of STAT3 Signaling Pathway by Morusin Induces Apoptosis and Inhibits Invasion in Human Pancreatic Tumor Cells. *Pancreas.* 2016;45(3):409–19.
43. Yin XL, Lv Y, Wang S, Zhang YQ. Morusin suppresses A549 cell migration and induces cell apoptosis by downregulating the expression of COX-2 and VEGF genes. *Oncol Rep.* 2018;40(1):504–10.
44. Wang J, Liu X, Zheng H, Liu Q, Zhang H, Wang X, Shen T, Wang S, Ren D. Morusin induces apoptosis and autophagy via JNK, ERK and PI3K/Akt signaling in human lung carcinoma cells. *Chem Biol Interact.* 2020;331: 109279.
45. Xue J, Li R, Zhao X, Ma C, Lv X, Liu L, Liu P. Morusin induces paraptosis-like cell death through mitochondrial calcium overload and dysfunction in epithelial ovarian cancer. *Chem Biol Interact.* 2018;283:59–74.
46. Jia Y, He W, Zhang H, He L, Wang Y, Zhang T, Peng J, Sun P, Qian Y. Morusin Ameliorates IL-1 β -Induced Chondrocyte Inflammation and Osteoarthritis via NF- κ B Signal Pathway. *Drug Des Dev Ther.* 2020;14:1227–40.
47. Cho AR, Park WY, Lee HJ, Sim DY, Im E, Park JE, Ahn CH, Shim BS, Kim SH. Antitumor Effect of Morusin via G1 Arrest and Antigliocolysis by AMPK Activation in Hepatocellular Cancer. *Int J Mol Sci.* 2021;22(19).
48. Thallinger C, Werzowa J, Poeppl W, Kovar FM, Pratscher B, Valent P, Quehenberger P, Joukhadar C. Comparison of a treatment strategy combining CCI-779 plus DTIC versus DTIC monotherapy in human melanoma in SCID mice. *J Invest Dermatol.* 2007;127(10):2411–7.
49. Schadendorf D, Ugurel S, Schuler-Thurner B, Nestle FO, Enk A, Bröcker EB, Grabbe S, Rittgen W, Edler L, Sucker A, et al. Dacarbazine (DTIC) versus vaccination with autologous peptide-pulsed dendritic cells (DC) in first-line treatment of patients with metastatic melanoma: a randomized phase III trial of the DC study group of the DeCOG. *Annals of oncology : official journal of the European Society for Medical Oncology.* 2006;17(4):563–70.
50. Lee MR, Kim JE, Choi JY, Park JJ, Kim HR, Song BR, Park JW, Kang MJ, Choi YW, Kim KM, et al. Morusin Functions as a Lipogenesis Inhibitor as Well as a Lipolysis Stimulator in Differentiated 3T3-L1 and Primary Adipocytes. *Mol.* 2018;23(8).
51. Lacroix M, Riscal R, Arena G, Linares LK, Le Cam L. Metabolic functions of the tumor suppressor p53: Implications in normal physiology, metabolic disorders, and cancer. *Mol Metab.* 2020;33:2–22.
52. Machado-Silva A, Perrier S, Bourdon JC. p53 family members in cancer diagnosis and treatment. *Semin Cancer Biol.* 2010;20(1):57–62.
53. Lim SL, Park SY, Kang S, Park D, Kim SH, Um JY, Jang HJ, Lee JH, Jeong CH, Jang JH, et al. Morusin induces cell death through inactivating STAT3 signaling in prostate cancer cells. *Am J Cancer Res.* 2015;5(1):289–99.
54. Zhang Y, Weng Q, Chen J, Han J. Morusin Inhibits Human Osteosarcoma via the PI3K-AKT Signaling Pathway. *Curr Pharm Biotechnol.* 2020;21(13):1402–9.
55. Li H, Wang Q, Dong L, Liu C, Sun Z, Gao L, Wang X. Morusin suppresses breast cancer cell growth in vitro and in vivo through C/EBP β and PPAR γ mediated lipoapoptosis. *J Exp Clin Cancer Res.* 2015;34:137.
56. Guo H, Liu C, Yang L, Dong L, Wang L, Wang Q, Li H, Zhang J, Lin P, Wang X. Morusin inhibits glioblastoma stem cell growth in vitro and in vivo through stemness attenuation, adipocyte transdifferentiation, and apoptosis induction. *Mol Carcinog.* 2016;55(1):77–89.
57. Nakamura Y, Fujisawa Y. Diagnosis and Management of Acral Lentiginous Melanoma. *Curr Treat Options Oncol.* 2018;19(8):42.
58. Gadducci A, Carinelli S, Guerrieri ME, Aletti GD. Melanoma of the lower genital tract: Prognostic factors and treatment modalities. *Gynecol Oncol.* 2018;150(1):180–9.
59. Morton DL, Thompson JF, Cochran AJ, Mozzillo N, Nieweg OE, Roses DF, Hoekstra HJ, Karakousis CP, Puleo CA, Coventry BJ, et al. Final trial report of sentinel-node biopsy versus nodal observation in melanoma. *N Engl J Med.* 2014;370(7):599–609.
60. Relecom A, Merhi M, Inchakalody V, Uddin S, Rinchai D, Bedognetti D, Dermime S. Emerging dynamics pathways of response and resistance to PD-1 and CTLA-4 blockade: tackling uncertainty by confronting complexity. *Journal of experimental & clinical cancer research : CR.* 2021;40(1):74.
61. Jia XH, Geng LY, Jiang PP, Xu H, Nan KJ, Yao Y, Jiang LL, Sun H, Qin TJ, Guo H. The biomarkers related to immune related adverse events caused by immune checkpoint inhibitors. *Journal of experimental & clinical cancer research : CR.* 2020;39(1):284.
62. Lemaire V, Shemesh CS, Rotte A. Pharmacology-based ranking of anti-cancer drugs to guide clinical development of cancer immunotherapy combinations. *Journal of experimental & clinical cancer research : CR.* 2021;40(1):311.
63. Zhang H, Dai Z, Wu W, Wang Z, Zhang N, Zhang L, Zeng WJ, Liu Z, Cheng Q. Regulatory mechanisms of immune checkpoints PD-L1 and CTLA-4 in cancer. *Journal of experimental & clinical cancer research : CR.* 2021;40(1):184.
64. Vafaei S, Zekiy AO, Khanamir RA, Zaman BA, Ghayourvahdat A, Azimi-zonuzi H, Zamani M. Combination therapy with immune checkpoint inhibitors (ICIs); a new frontier. *Cancer Cell Int.* 2022;22(1):2.
65. Duffy MJ, Synnott NC, Crown J. Mutant p53 as a target for cancer treatment. *Eur J Cancer (Oxford, England : 1990).* 2017;83:258–65.
66. Thiem A, Hesbacher S, Kneitz H, di Primio T, Heppert MV, Hermanns HM, Goebeler M, Meierjohann S, Houben R, Schrama D. IFN- γ -induced PD-L1 expression in melanoma depends on p53 expression. *Journal of experimental & clinical cancer research : CR.* 2019;38(1):397.

67. Hodi FS, Chiarion-Sileni V, Gonzalez R, Grob JJ, Rutkowski P, Cowey CL, Lao CD, Schadendorf D, Wagstaff J, Dummer R, et al. Nivolumab plus ipilimumab or nivolumab alone versus ipilimumab alone in advanced melanoma (CheckMate 067): 4-year outcomes of a multicentre, randomised, phase 3 trial. *Lancet Oncol*. 2018;19(11):1480–92.
68. Larkin J, Chiarion-Sileni V, Gonzalez R, Grob JJ, Rutkowski P, Lao CD, Cowey CL, Schadendorf D, Wagstaff J, Dummer R, et al. Five-Year Survival with Combined Nivolumab and Ipilimumab in Advanced Melanoma. *N Engl J Med*. 2019;381(16):1535–46.
69. Kastan MB, Onyekwere O, Sidransky D, Vogelstein B, Craig RW. Participation of p53 protein in the cellular response to DNA damage. *Cancer Res*. 1991;51(23 Pt 1):6304–11.
70. Miyashita T, Krajewski S, Krajewska M, Wang HG, Lin HK, Liebermann DA, Hoffman B, Reed JC. Tumor suppressor p53 is a regulator of bcl-2 and bax gene expression in vitro and in vivo. *Oncogene*. 1994;9(6):1799–805.
71. Güllülü Ö, Hehlhans S, Rödel C, Fokas E, Rödel F. Tumor Suppressor Protein p53 and Inhibitor of Apoptosis Proteins in Colorectal Cancer—A Promising Signaling Network for Therapeutic Interventions. *Cancers (Basel)*. 2021;13(4).
72. Cui H, Schroering A, Ding HF. p53 mediates DNA damaging drug-induced apoptosis through a caspase-9-dependent pathway in SH-SY5Y neuroblastoma cells. *Mol Cancer Ther*. 2002;1(9):679–86.
73. Ahmed MM, Venkatasubbarao K, Fruitwala SM, Muthukkumar S, Wood DP Jr, Sells SF, Mohiuddin M, Rangnekar VM. EGR-1 induction is required for maximal radiosensitivity in A375–C6 melanoma cells. *J Biol Chem*. 1996;271(46):29231–7.
74. Wu Z, Wu L, Li L, Tashiro S, Onodera S, Ikejima T. p53-mediated cell cycle arrest and apoptosis induced by shikonin via a caspase-9-dependent mechanism in human malignant melanoma A375–S2 cells. *J Pharmacol Sci*. 2004;94(2):166–76.

Publisher's Note

Springer Nature remains neutral with regard to jurisdictional claims in published maps and institutional affiliations.

Ready to submit your research? Choose BMC and benefit from:

- fast, convenient online submission
- thorough peer review by experienced researchers in your field
- rapid publication on acceptance
- support for research data, including large and complex data types
- gold Open Access which fosters wider collaboration and increased citations
- maximum visibility for your research: over 100M website views per year

At BMC, research is always in progress.

Learn more biomedcentral.com/submissions

